Harmonic Filters Influences Regarding the Power Quality on High Frequency Electrothermal Installation with Electromagnetic Induction

RALUCA ROB*, IOAN SORA**, CAIUS PANOIU*, MANUELA PANOIU*
* Polytechnic University of Timisoara, Faculty of Engineering Hunedoara
Revolutiei street, no 5, Hunedoara, cod 331115, Romania
{raluca.rob, c.panoiu, m.panoiu}@fih.upt.ro
** Polytechnic University of Timisoara, Faculty of Electrical Engineering
V. Pârvan street, no 2, Timişoara, cod 300223, Romania
isora@et.utt.ro

Abstract: - This paper presents a study regarding the functioning of a melting/hardening electrothermal installation with electromagnetic induction from the point of view of generated harmonics in the power distribution. The authors made simulations in scope of reducing the effects of the generated non-sinusoidal regime.

Key-Words: - Electrothermal installation, harmonic, static converter, passive filters.

1. Introduction

The harmonic voltages determined by the non-sinusoidal voltages sources and applied to the power distribution lead to the appearance of the same or different rank harmonic currents, witch are amplified by the nonlinear elements of the circuit.

The frequency converters that are used in electrothermal installation sources lead to negative effects in the power distribution:
- distortion of the voltage waveform in power distribution
- additional heating due to the rising of the current effective value
- improper functioning of the protection relays.

Electrothermal installation that is analyzed in this paper contains an inverter source supplied by a diode bridge rectifier. This type of nonlinear load is a voltage harmonic source. Although the current is deeply distorted, the harmonics amplitude is more influenced by the impedance of the power distribution, while the rectifier voltage is typically, being less dependent by the impedance of the power distribution.

2. Theoretical consideration

The main goal of this paper is to simulate the functioning of the electrothermal installation without and with power conditioning and to evaluate the energy quality at power distribution level.

The melting/hardening electrothermal installation is composed by a converter CTC 100K15 and two inductors: one designed for melting and one designed for hardening the materials. CTC 100K15 has the following electric characteristics:
- supplying voltage 3x400V, 50Hz
- rated current 27A
- control voltage 24Vdc
- consumed power at high frequency 15kW
- voltage at medium frequency 500Vac

In the next paragraphs are presented the containing elements of the converter presented in figure1.

2.1. General distribution board

The electrothermal installation is supplied from the three phase low voltage (0.4kV) through a general distribution board equipped with an automat circuit-breaker with thermal protection (Ir = 40A), electromagnetic protection (Iem=5It), differential protection (Id = 300mA) and overvoltage at 50Hz protection (U>=260-280V). By circuit-breaker releasing as a result of an anormal functioning regime, it is realised the separation of the faulted part from the rest of the instalation, following the limitation of the fault development that can be transformed to a general breakdown. The overload and the electromagnetic protection are maximal current protections and they are acting at the presence of an overload in the protected circuit. They are realised with current relays witch are acting when the current exceeds a thershold value. The differential protection works when appears a phasorial difference between the currents from the edges of the protected zone. In normal functioning, these currents are considered equals and in phase.

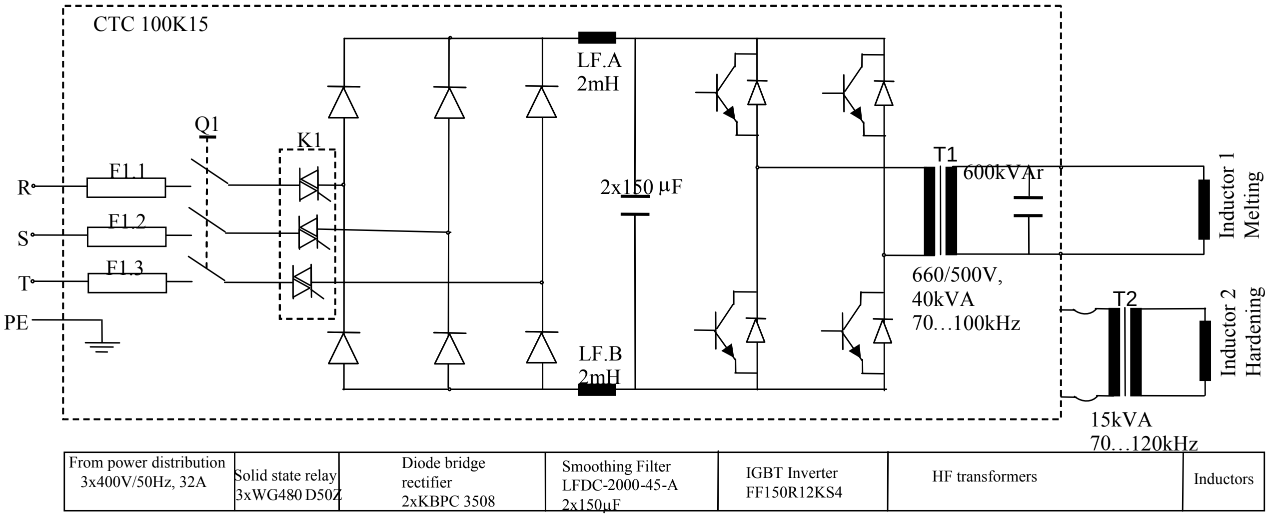

Fig.1. Melting/hardening electrothermal installation.

If is appreaing a fault in the outside of protected area, the values of these currents are incresed, but the difference is still zero. If the fault is inside of protected area, the phase is modified.

Through the relay is circulating the phasorial difference of these currents, and the protection is working at a prescribed value. The voltage maximal protection is responding at a rising of the circuit voltage.

2.2. Solid state relay SSR

The on/off switching of the installation is made with three static contactors WG480-D50Z (Solid state relay-SSR). Like all relays, the SSR requires relatively low control circuit energy to switch the output state from off to on, or vice versa. Since this control energy is very much lower than the output power controllable by the relay at full load, "power gain" in an SSR is substantial--frequently much higher than in an electromagnetic relay of comparable output rating. Photo-coupled SSR's (figure 2), in which the control signal is applied to a light or infrared source (usually, a light-emitting diode, or LED), detected the radiation from that source in a photosensitive semi-conductor (i.e., a photosensitive diode, a photo-sensitive transistor, or a photo-sensitive thyristor). The output of the photo-sensitive device is then used to trigger (gate) the TRIAC that switch the load current. Clearly, the only significant "coupling path" between input and output is the beam of light or infrared radiation, and electrical isolation is excellent. These SSR's are also referred to as "optically coupled" or "photo-isolated".

Input characteristics:
- dielectric strength: 1500Vac
- insulation resistance: 10^3-10^6MΩ
- stray capacitance: 1-10pF

Output circuit performance:

The most significant output-circuit parameters are the maximum load-circuit voltage that may be impressed across the relay output circuit in the off condition without causing it to break down into conduction or failure, and the maximum current that can flow through the output circuit and load in on condition.

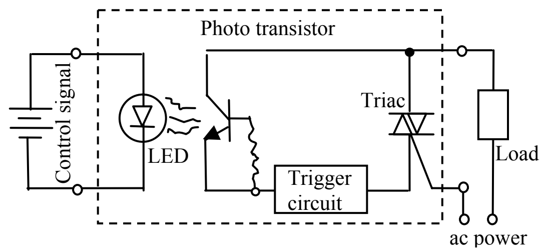

Fig.2. Photo-coupled SSR.

2.3. Diode bridge rectifier

In the electric scheme are introduced two diode bridge rectifiers KBPC 3508 with the following electric characteristics:
-maximum recurrent peak reverse voltage 800V
-maximum rms bridge input voltage 560V
-maximum average forward rectified output current 35A
-peak forward surge current 8.3ms single-half sine-wave superimposed on rated load 400A
-maximum forward voltage drop per element 1.2V
-maximum reverse current at rated dc blocking voltage per element 1μA.

The bridge rectifiers are composed of two commutation cells with median point. The diode of positive cell that has the anode at the highest positive potential will conduct and will transmit the potential of its phase to positive terminal. The potential of the positive terminal follows the positive curve of the three phase voltage system. Similarly, it will conduct the diode of the negative cell that has the cathode at the lowest negative potential. The potential of the negative terminal follows the negative curve of the three phase voltage system.

For each commutation cell, the diode conduction angle is 120°. The rectified voltage is obtained by the potential difference between the positive and the negative terminals. At the output of the rectifier is obtained a 6 pulses rectified voltage. The secondary voltages are:

$$u_A = U_S^{'} \sin \omega t, \qquad u_B = U_S^{'} \sin\left(\omega t - \frac{2\pi}{3}\right),$$

$$u_C = U_S^{'} \sin\left(\omega t + \frac{2\pi}{3}\right) \qquad (1)$$

where $U_S^{'}$ is the peak value of U_S voltage.

For damping the rectified voltage pulsations, the electrothermal installation contains a smoothing filter LFDC-2000-45-A. The inductance permits the passing of the continuous component and the whole continuous current from the inductance output is crossing the load. The alternative component is blocked by the inductance and the whole alternative current that cross the inductance is passing through the capacitor.

2.4. Inverter

In order to control the frequency in the melting and hardening process, it is using an inverter with IGBT transistors: FF150R12KS4.

The IGBT structure consists in a modified Darlington connection. It has two transistors: a PNP bipolar power transistor and a MOS transistor. The conduction and the breakdown states of an IGBT transistor are controlled with a positive voltage applied to the gate terminal. The FF150R12KS4 inverter has the following characteristics:

-collector-emitter breakdown voltage 1200V
-collector-emitter saturation voltage 3,2V
-continuous collector current I_{Cmax} 225A
-gate-emitter leakage current 400nA
-power disipation 1,25kW

2.5. High frequency transformers

For supplying the melting and hardening inductors there are two high frequency toroidal transformers:

-melting: 660/500V, 40kVA, 70-100kHz.
-hardening: 500/500V, 15kVA, 70-120kHz.

Figure 3 presents the equivalent scheme of the windings.

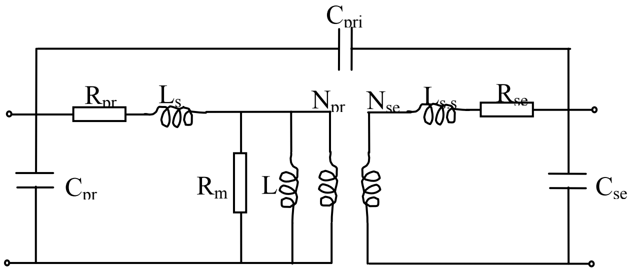

Fig.3. Equivalent scheme of the windings.

The authors used the following notations:
N_{prim} = number of primary turns
N_{sec} = number of secondary turns
R_{miez} = core loss resistance
R_{prim} = primary resistance
R_{sec} = secondary resistance
L_m = magnetizing inductance
$L_{s.prim}$ = primary leakage inductance
$L_{s.sec}$ = secondary leakage inductance
C_{prim} = primary intrawinding capacitance
C_{sec} = secondary intrawinding capacitance
$C_{prim \cdot sec}$ = primary to secondary capacitance

The transformer core is made of ferrite that constitutes the most suitable material in core designing at frequency of 10 kHz - 50 MHz range due to optimal combination of low cost, high quality, good stability and reduced volume.

In figure 4 are used the following notations:
A_C is the core area
A_W is the winding area
l_C is the core lenght
l_W is the average winding turn lenght

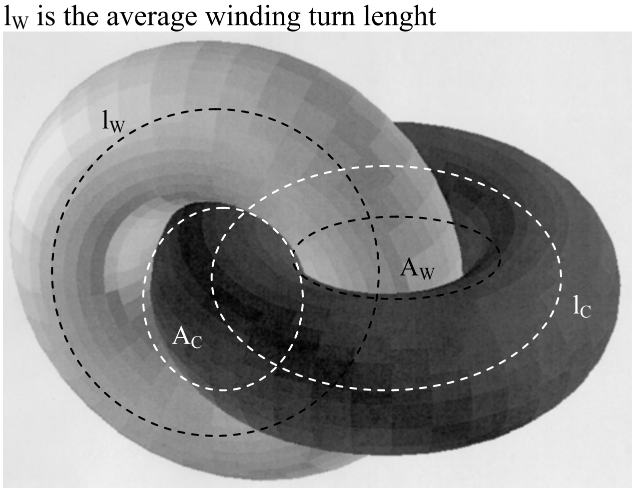

Fig.4. High frequency toroidal transformer.

Ferrites are compounds of some metals (Mn, Zn, Ni or Mg) with iron oxides (Fe_2O_3) and have some advantages in comparison with other magnetic materials: high electric resistivity and magnetic permeability and reduced loss in a large frequency range.

In HF transformers designing it must be taken into consideration the followings: hysteresis core losses, eddy current core losses, load current winding losses, magnetizing current winding losses, winding parasitics, temperature rise.

2.6. Inductors

The electrothermal installation contains two inductors : one for melting and one for hardening process, following the electromagnetic induction heating principle: a winding that is crossed by alternative current will create a variable magnetic field that pass the material determining eddy currents that are heating the material. In order to measure the electromagnetic energy crossing, it is using the crossing depth δ . This represents the distance from material surface in witch, due to pelicular effect, the current density is decreasing by e = 2,71 times, and the active power by e^2 times. In this layer 86,5% of active power from the surface of the material is converting in heating.

Induction heating electric efficiency η_e depends on the effective power and the total consumed power like in the relation:

$$\eta_e = \frac{1}{1 + P_1/P_2} \qquad (2)$$

where $P_2 = R_2 I_2^2$ is the received power and $P_1 = R_1 I_1^2$ is dissipated power through Joule effect [1];

R_1 and R_2 are the electric resistance of inductor, respectively of piece.

The crossing depth is given by the relation:

$$\delta = \sqrt{\frac{2\rho}{\omega\mu}} = 503\sqrt{\frac{\rho}{\mu_r f}} \text{ [m]} \qquad (3)$$

where $\omega = 2\pi f$ is the current pulsation.

$\mu = \mu_0 \mu_r = 4\pi \cdot 10^{-7}$

μ_0 [H/m] is absolute permeability

μ_r is relative permeability

As it can be seen from the above relation, the crossing depth depend on frequency, material and temperature. The melting furnaces or the heating instalations are supplied on low frequency because they need a high value for crossing depth. In opposite side, the superficial thermal treatments installations are supplied on higher frequencies.

3. Passive filters

The classic solutions in order to reduce the distortion regime are based on using the passive components.

In this paper the authors use a few of the common passive filters to reduce the distortion effect introduced by the electrothermal installation in the power system: a Parallel Passive Filter, a Series Passive Filter, and a Low-Pass Passive Filter.

3.1. Parallel Passive Filter

This type of passive filter is composed by a series of an inductance and a capacitance, as in figure 5, accorded on the frequency of the harmonic whose magnitude must be reduced, in order to respect the Thompson relation [2]:

$$f_n = \frac{1}{2\pi\sqrt{LC}} \qquad (4)$$

This LC filter is connected in parallel with the harmonic source, being a minimum impedance block, in order to shunt the current harmonics.

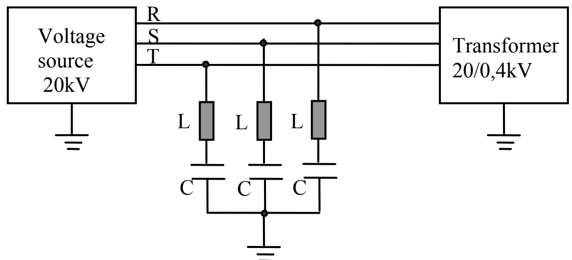

Fig.5. Parallel passive filter.

There was studied the variation of the 5^{th}, 7^{th}, 11^{th} and 13^{th} order harmonic currents of the installation without filters.

According to relation (4), the authors calculate the parallel passive filter for each studied harmonic current.

The filtering evolution was followed using four parallel passive filters:

n = 5; fn = 250Hz; L = 0.01243H; C = 32.605μF
n = 7; fn = 350Hz; L = 0.01243H; C = 16.622μF
n = 11; fn = 550Hz; L = 0.01243H; C = 6.736μF
n = 13; fn = 650Hz; L = 0.01243H; C = 4.823μF

3.2. Series Passive Filter

The series passive filter consists in LC parallel circuits accorded on the frequency of the current harmonics that must be rejected from the harmonic source. This LC group is connected in series with the harmonic source, as in figure 6. The filter represents a maximal impedance block, obstructioning the harmonic currents to penetrate the power distribution network.

With respect to the relation (4), the authors calculate four series passive filters:

n = 5; fn = 250Hz; R = 1kΩ; L = 0.01243H; C = 32.605μF
n = 7; fn = 350Hz; R = 1kΩ; L = 0.01243H; C = 16.622μF

n = 11; fn = 550Hz; R = 1kΩ; L = 0.01243H; C = 6.736μF
n = 13; fn = 650Hz; R = 1kΩ; L = 0.01243H; C = 4.823μF

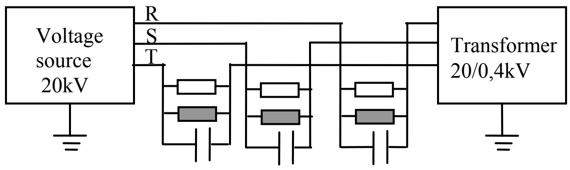

Fig.6. Series passive filter.

3.3. Low-Pass Passive Filter

This type of filter consists in two series inductances with equal values and a capacitance connected in parallel with the harmonic source, as in figure 7. The filtering evolution was followed using four LCL filters:

n = 5; fn = 250Hz; $L_{1,2}$ = 0.25H; C = 1.6211μF
n = 7; fn = 350Hz; $L_{1,2}$ = 0.25H; C = 0.8271μF
n = 11; fn = 550Hz; $L_{1,2}$ = 0.25H; C = 0.3349μF
n = 13; fn = 650Hz; $L_{1,2}$ = 0.25H; C = 0.2398μF

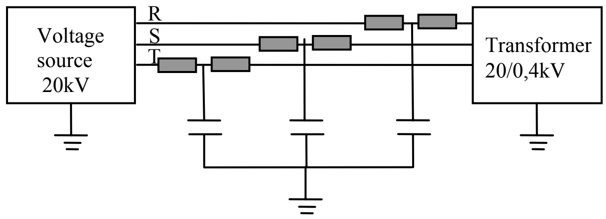

Fig.7. Low-pass passive filter.

Figure 8 presents the simulated scheme of the electrothermal installation with electromagnetic induction without filters.

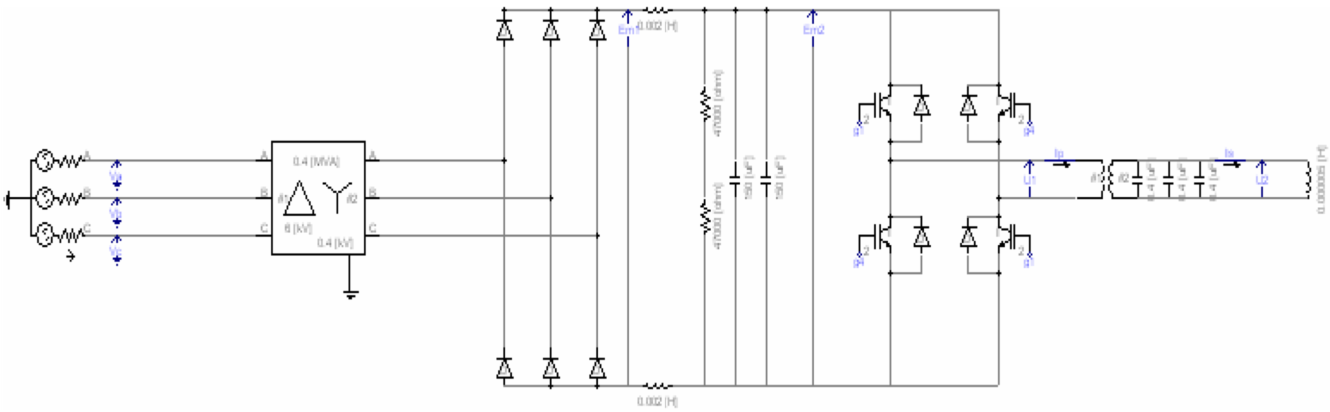

Fig.8. Simulated scheme of the electrothermal installation.

4. Simulation in PSCAD-EMTDC

PSCAD-EMTDC tool was used to develop the simulation of the electrothermal installation.

In scheme from figure 4 there were used the following notations:

-I_{Sa}, I_{Sb}, I_{Sc} are the source currents
-I_a, I_b, I_c are the load currents

In order to study the current harmonics, the authors use a Fast Fourier Transformation analyzer, and a harmonic distortion calculator according to the below relation (5):

$$THD = \sqrt{\sum_{k=2}^{n} \left(\frac{F_k}{F_1} \right)^2} \cdot 100\,[\%] \qquad (5)$$

where n is a given by the number of harmonics input paramaters.

4.1. Simulation of the installation without filters

In figure 9 are presented the source and the load currents and figure 10 shows the THD for electrothermal installation without filters.

Figure 11 presents the variation of the 5^{th}, 7^{th}, 11^{th} and 13^{th} order source harmonic currents of the installation without filters and below the load harmonic currents.

4.2. Simulation of the installation using parallel passive filter

In the followings, the authors present the simulation results using an LC shunt passive filter accorded on the 5th harmonic frequency (f=250Hz). Figure 12 shows the source and the load currents for described situation and figure 13 presents total harmonic distortion obtained by simulations.

Figure 14 presents the variation of the 5^{th}, 7^{th}, 11^{th} and 13^{th} order source and load harmonic currents of the installation using an LC shunt passive filter accorded on f=250Hz (5^{th} harmonic).

The simulations were made using LC shunt passive filters for each harmonic: 5^{th}, 7^{th}, 11^{th} and 13^{th} order.

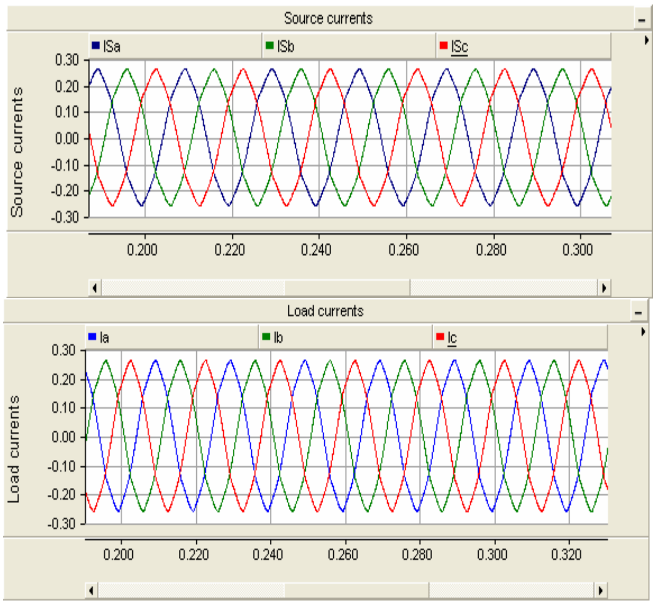

Fig.9. Source and load currents for nonfiltered installation.

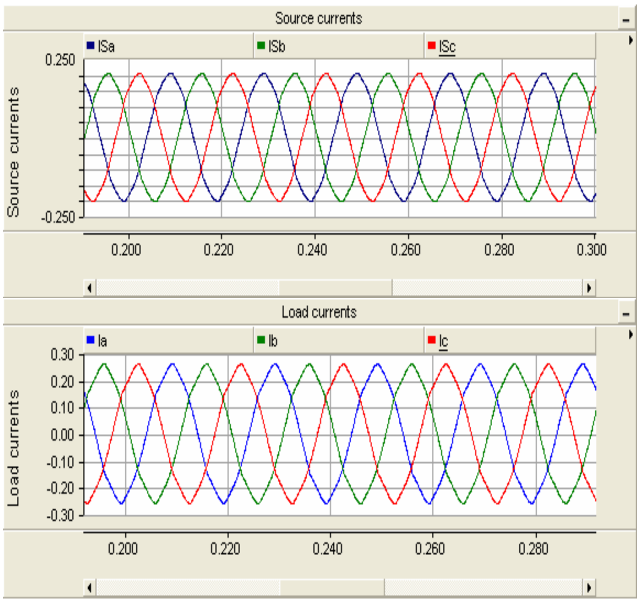

Fig.12. Source and load currents using LC shunt passive filter (5th harmonic).

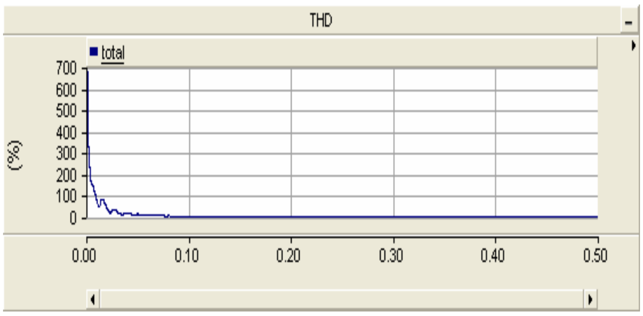

Fig.10. Total harmonic distortion in nonfiltered installation.

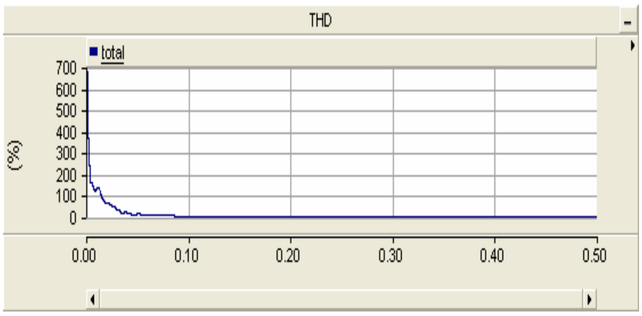

Fig.13. Total harmonic distortion using 5th harmonic filter.

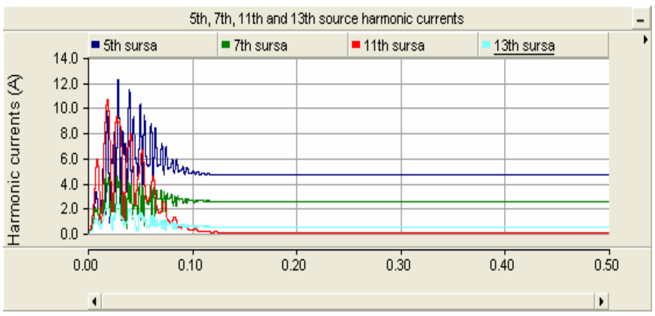

Fig.11a). Harmonic source currents in nonfiltered installation.

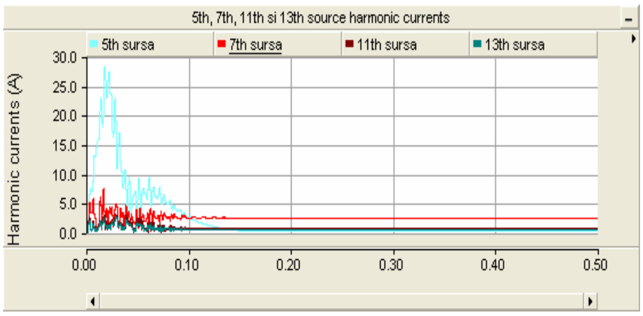

Fig.14a). Harmonic source currents using LC shunt passive filter (5^{th} harmonic).

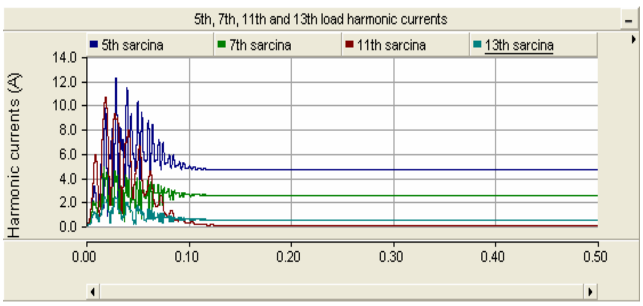

Fig.11b). Harmonic load currents in nonfiltered installation.

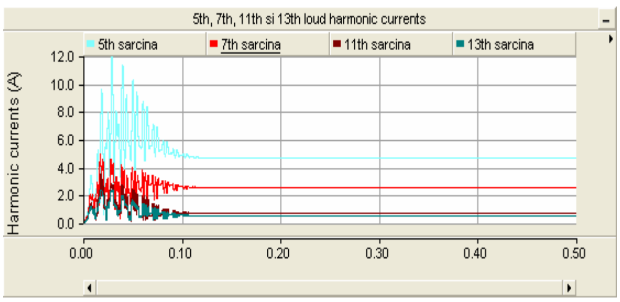

Fig.14b). Harmonic load currents using LC shunt passive filter (5^{th} harmonic).

4.3. Simulation of the installation using series passive filter

Figure 15 presents the source and load currents for the electrothermal installation using a series passive filter composed by a LC parallel group connected in series with the harmonic source.

Total harmonic distortion for the installation using series passive filter is presented in figure 16.

The harmonic source and load currents for the installation using series passive filter are presented in figure 17.

4.4. Simulation of the installation using low-pass passive filter

Figure 18 presents the source and load currents for the electrothermal installation using a low-pass passive filter composed by two series inductances and a capacitance connected in parallel with the harmonic source.

Total harmonic distortion for the installation using low-pass passive filter is presented in fig.19.

The harmonic source and load currents for the installation using series passive filter are presented in fig.20.

4.5. Simulation of the installation using parallel passive filters for all studied harmonic currents

In order to reduce the harmonic effect, the authors investigate the situation of using parallel passive filters for all studied harmonic currents:

-parallel passive filters for 5th, 7th, 11th and 13th harmonic currents.

Figure 21 presents the source and load currents for the electrothermal installation using the four parallel passive filters.

Total harmonic distortion for the installation using four parallel passive filters is presented in fig.22.

The harmonic source and load currents for the installation using four parallel passive filter are presented in fig.23.

Figure 24 presents the scheme of the installation source with this type of filters.

In the following figures the authors noted with I_{Sa}, I_{Sb}, I_{Sc} the source currents, and with I_a, I_b, I_c the load currents. The installation is supplied by a triphased fixed voltage source with the following parameters: line voltage Un = 6kV, frequency f = 50Hz, internal resistance r = 1Ω.

The power transformer has the following electric characteristics: the line votages Un = 6 / 0.4kV, apparent power Sn = 0,4MVA, frequency f = 50Hz, the primary winding is in Δ connection, the secondary winding is in Y connection.

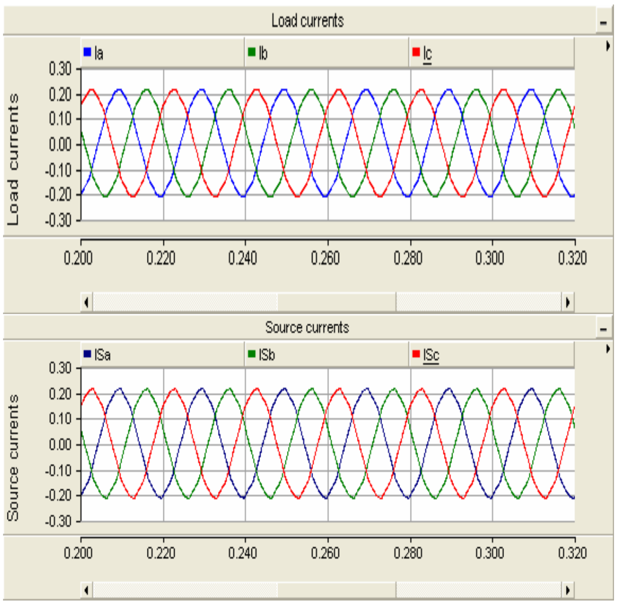

Fig.15. Source and load currents for installation using series passive filter.

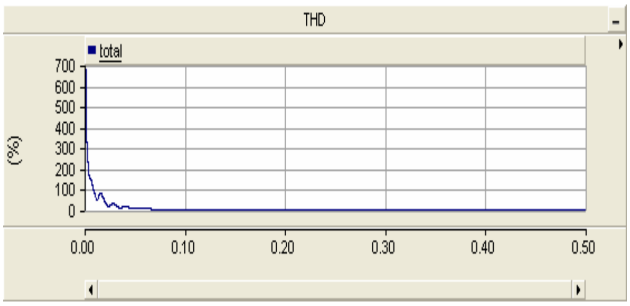

Fig.16. Total harmonic distortion in installation with series passive filter.

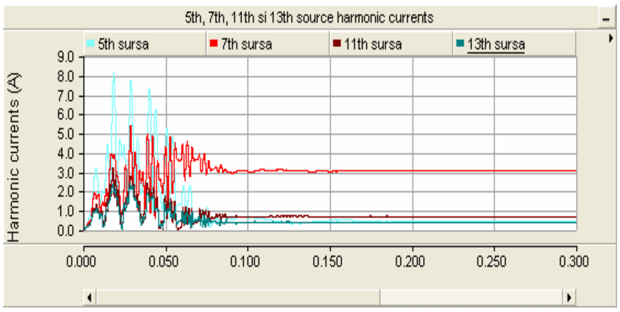

Fig.17a) Harmonic source currents for installation using series passive filter.

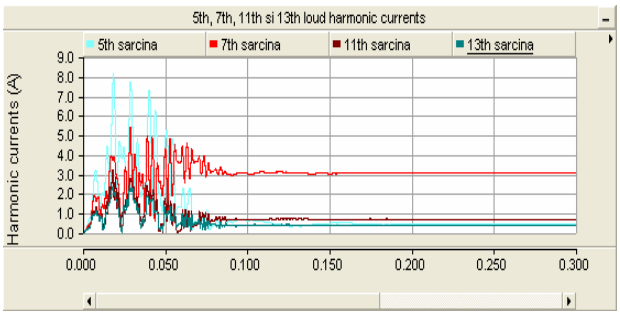

Fig.17b). Harmonic load currents for installation with series passive filter.

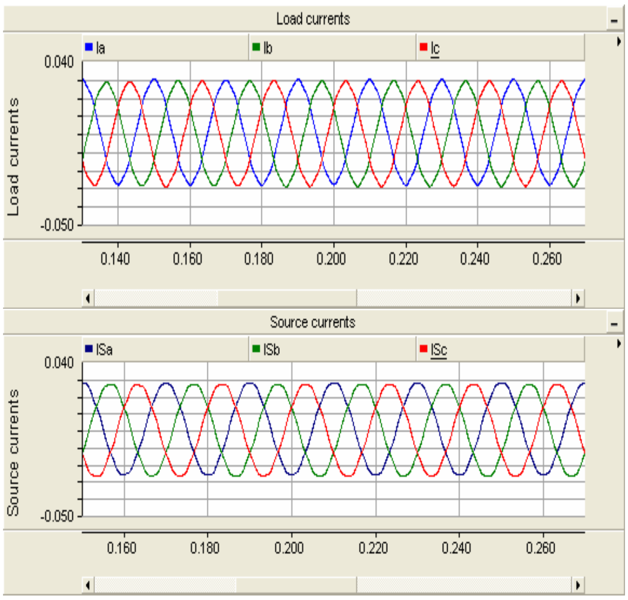

Fig.18. Source and load currents for installation using low-pass passive filter.

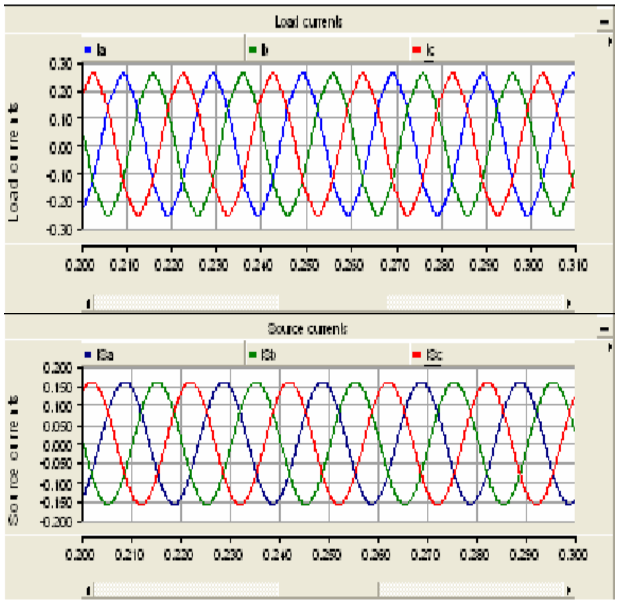

Fig.21. Source and load currents for installation using all studied parallel passive filter.

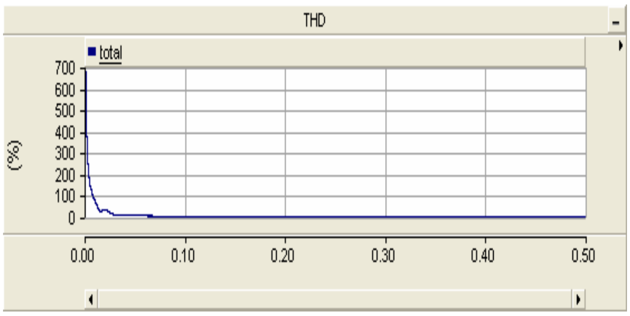

Fig.19. Total harmonic distortion in installation with low-pass passive filter.

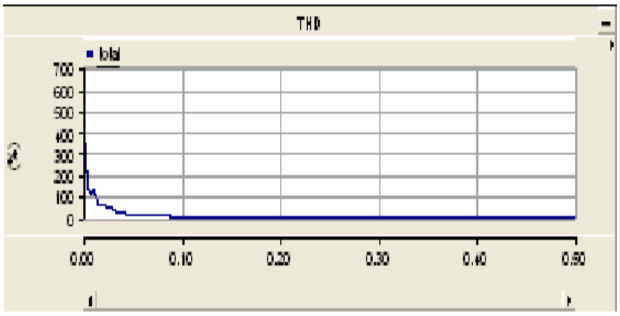

Fig.22. Total harmonic distortion in installation with four parallel passive filter.

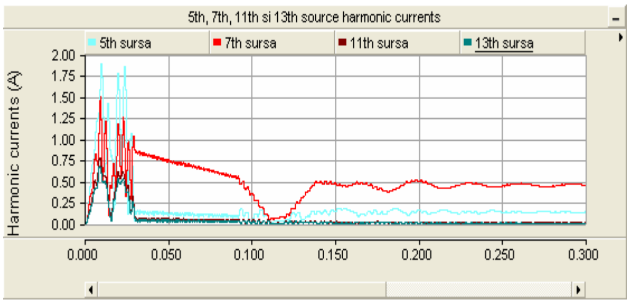

Fig.20a). Harmonic source currents for installation with low-pass passive filter.

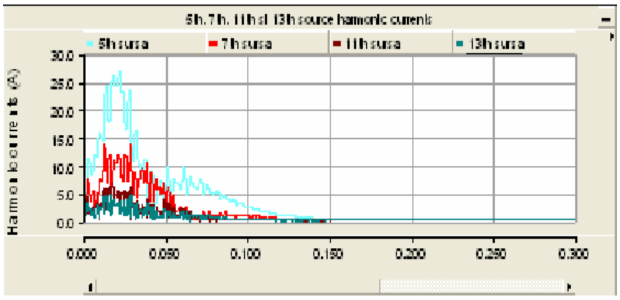

Fig.23a). Harmonic source currents for installation with all studied parallel passive filter.

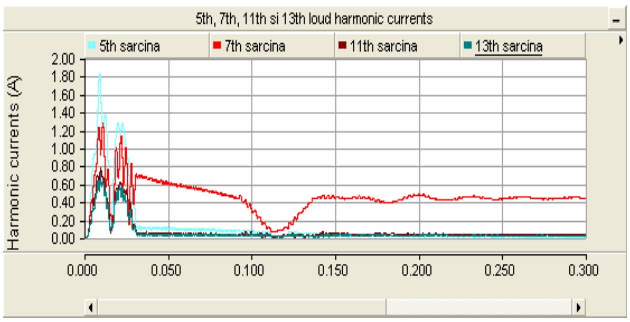

Fig.20b). Harmonic load currents for installation with low-pass passive filter.

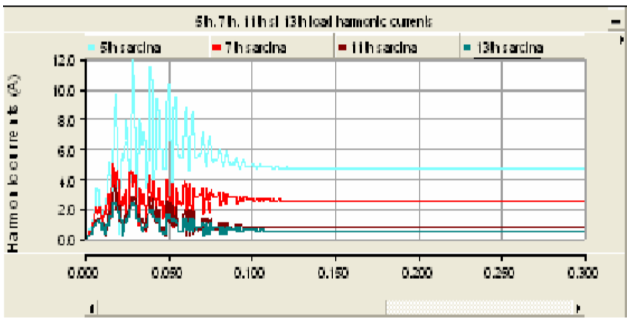

Fig.23b). Harmonic load currents for installation with all studied parallel passive filter.

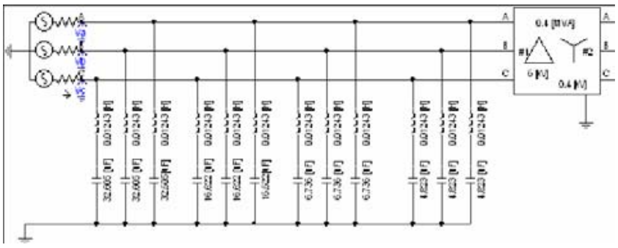

Fig.21. Parallel passive filter for all studied harmonics.

5. Results and conclusions

Studying the resulting simulations, the output data completes the following table:

5.1 Parallel passive filter

Harmonic order	Without filters (A)	With 5th harmonic filter (A)	With 7th harmonic filter (A)	With 11th harmonic filter (A)	With 13th harmonic filter (A)
5	4.603	**0.186**	4.599	4.600	4.600
7	2.503	2.494	**0.185**	2.501	2.502
11	0.671	0.674	0.670	**0.158**	0.668
13	0.488	0.490	0.489	0.487	**0.167**
THD (%)	**3.823**	**1.900**	**2.964**	**3.123**	**3.099**

It can be observed that:
-in case of using 5th harmonic filter, the magnitude of the 5th harmonic current is decreasing from 4.603A to 0.186A (THD=1.900%)
-in case of using 7th harmonic filter, the magnitude of the 7th harmonic current is decreasing from 2.503A to 0.185A (THD=2.964%).
-in case of using 11th harmonic filter, the magnitude of the 11th harmonic current is decreasing from 0.671A to 0.158A (THD=3.123%).
-in case of using 13th harmonic filter, the magnitude of the 13th harmonic current is decreasing from 0.488A to 0.167A (THD=3.099%).

5.2 Series passive filter

It can be observed that:
-in case of using 5th harmonic filter, the magnitude of the 5th harmonic current is decreasing from 4.603A to 0.421A (THD=2.160%)
-in case of using 7th harmonic filter, the magnitude of the 7th harmonic current is decreasing from 2.503A to 0.375A (THD=2.203%).
-in case of using 11th harmonic filter, the magnitude of the 11th harmonic current is decreasing from 0.671A to 0.648A (THD=3.015%).
-in case of using 13th harmonic filter, the magnitude of the 13th harmonic current is decreasing from 0.488A to 0.472A (THD=3.014%).

Harmonic order	Without filters (A)	With 5th harmonic filter (A)	With 7th harmonic filter (A)	With 11th harmonic filter (A)	With 13th harmonic filter (A)
5	4.603	**0.421**	3.024	4.469	4.469
7	2.503	3.038	**0.375**	2.430	2.430
11	0.671	0.683	0.989	**0.648**	0.648
13	0.488	0.379	0.478	0.472	**0.472**
THD (%)	**3.823**	**2.160**	**2.203**	**3.015**	**3.014**

5.3 Low-pass passive filter

Harmonic order	Without filters (A)	With 5th harmonic filter (A)	With 7th harmonic filter (A)	With 11th harmonic filter (A)	With 13th harmonic filter (A)
5	4.603	**0.140**	0.096	0.081	0.080
7	2.503	0.452	**0.103**	0.063	0.062
11	0.671	0.008	0.060	**0.058**	0.049
13	0.488	0.003	0.016	0.086	**0.052**
THD (%)	**3.823**	**2.473**	**0.796**	**0.768**	**1.797**

It can be observed that:
-in case of using 5th harmonic filter, the magnitude of the 5th harmonic current is decreasing from 4.603A to 0.140A (THD=2.473%)
-in case of using 7th harmonic filter, the magnitude of the 7th harmonic current is decreasing from 2.503A to 0.103A (THD=0.796%).
-in case of using 11th harmonic filter, the magnitude of the 11th harmonic current is decreasing from 0.671A to 0.058A (THD=0.768%).

-in case of using 13th harmonic filter, the magnitude of the 13th harmonic current is decreasing from 0.488A to 0.052A (THD=1.797%).

5.4 Four parallel passive filter

Harmonic order	Without filters (A)	With all studied passive filters (A)
5	4.603	0.176
7	2.503	0.192
11	0.671	0.151
13	0.488	0.156
THD (%)	3.823	0.548

It can be observed that in case of using all studied passive filter, the magnitude of 5th harmonic current is decreasing from 4.603A to 0.176A, the magnitude of 7th harmonic current is decreasing from 2.503A to 0.192A, the magnitude of 11th harmonic current is decreasing from 0.671A to 0.151A, the magnitude of 13th harmonic current is decreasing from 0.488A to 0.156A.

References

[1] N. Golovanov, I. Şora ş.a., *Electro-thermia and electro-technologies*, Tehnical publishing, Bucureşti, 1997

[2] A. Hedes, I. Sora, *Echipamente cu inalta frecventa pentru sudarea cu arc electric*, Ed.Orizonturi universitare Timisoara, 2001

[3] Sippola, Mika, *Developments for the high frequency power transformer. Design and implementation,* Electronic Publications E3 Espoo 2003.

[4] Iagar A, Popa GN, Dinis CM, *Power Quality Measurement for Line Frequency Coreless Induction Furnaces in MV Network*, Proceedings of the 8th WSEAS International Conference On Electric Power Systems, High Voltages, Electric Machines, Pages: 153-158

[5] Pănoiu, M., Pănoiu, C., *Modelarea si simularea proceselor neliniare in electrotermie*, Ed. Mirton, Timisoara 2008

[6] SC AAGES Ltd. Târgu Mureş, *Transistor based frequency converter type CTC 100K15. Electrical documentation*

[7] Pănoiu Manuela, Pănoiu Caius, Şora Ioan, Iordan Anca, Rob Raluca, *Using simulation for study the posibility of cancelling load unbalance of non-sinusoidal high power three phase loads*, WSEAS Transaction on Systems, vol.7, pag. 699-710, 2008.

[8] Pănoiu Manuela, Pănoiu Caius, Osaci Mihaela, Muscalagiu Ionel, *Simulation result about harmonics filtering using measurment of some electrical items in electrical installation on UHP EAF*, WSEAS Transaction on Circuits and Systems, vol.7, pag. 22-31, 2008.